Presented at SDG Short Course I on Exploration and Development of Geothermal Resources,
organized by UNU-GTP, GDC and KenGen, at Lake Bogoria and Lake Naivasha, Kenya, Nov. 10-31, 2016.

APPLICATION OF MICRO-SEISMIC METHODS TO GEOTHERMAL EXPLORATION: EXAMPLES FROM THE KENYA RIFT

Silas M. Simiyu
Kenya Electricity Generating Company Ltd. (KenGen)
P.O. Box 785, Naivasha
KENYA
ssimiyu@kengen.co.ke

ABSTRACT

Results from volcano-seismic studies of many geothermal fields show that they are possible resource-mapping tools for geothermal exploration and reservoir monitoring. They have been able to map the size and depth of possible shallow geothermal heat sources by analyzing data for seismic gaps, S-wave attenuation, reflected arrivals and converted waves. Analysis of shear wave split data for fracture density show high permeability areas that are potential targets for drilling high-producer wells. Variation of Vp/Vs ratios is related to reservoir fluid phases where low values are related to a decrease in P-wave velocity in the area with low pore pressure, high heat flow, fracturing and steam/gas saturation in the reservoir. High velocity ratios were found in the relatively liquid-saturated high-pressure fields that these ratios are useful tools for monitoring reservoirs under exploitation. The volcano-seismic approach can be useful as a stand alone tool for analyzing geothermal resource both at the exploration and exploitation stage that is cost effective in the long term

1. INTRODUCTION

The main objective of any scientific investigation for a geothermal resource is to locate a potentially attractive reservoir which can be economically exploited for electric power generation and other uses. Such indicators as a heat source, availability and characteristics of fluids, reservoir temperature and flow channels are the main parameters investigated. Most of these parameters are sometimes manifested on the surface whereas in other cases there are virtually no surface expressions though there is a resource lying underneath. To maximize on evaluation in the later 'blind resource' type of areas, different geological, geochemical and geophysical methods have been applied in various geothermal fields. Unlike in the oil industry where there are enormous financial resources, the geothermal industry has lacked the capacity to set up large seismic networks and develop techniques needed for resource evaluation using seismic methods.

However, numerous studies show that recent intrusions are associated with high levels of earthquake activity (e.g. Mt. St. Helen: Nevado del Ruiz, Lees, and Crosson, 1989, Zollweg, 1989; Fehler, 1983; Krafla, Iceland: Foulger, 1983; Stromboli, Italy: Ntepe and Dorel, 1990; Mammoth: Stroujkova & Malin, 1999). Spectral analysis of individual events shows that they are characterized by unique, low frequency source mechanisms. The events are often emergent, lack clear phases, and contain several characteristic frequencies. These events give information on the dimensions of their associated

magmatic and hydrothermal systems. In practical terms, these are the features that control the potential energy present in a given geothermal field.

A number of changes in the recent past have modified the capacity to use microearthquakes for geothermal studies. The cost of seismic instruments has been decreasing and the possibility of collaboration between institutions to work together by pooling resources including instruments has made it possible to carry out such studies.

Recent studies have focussed on the use of natural earthquake activity as a tool for geothermal evaluation of the heat source, fluid flow channels-permeability and reservoir properties. These are normally carried out following the objectives below:

a) Map the location of heat sources by using spatial seismic intensity, hypocenter distribution, shear wave attenuation and P wave reflection.
b) Map high crack density zones as an aide to siting high producer wells by inverting for three-dimensional crack direction and crack density in the target volume using the polarization angle.
c) Determine the fluid phase, reservoir size and characteristics by determining the variation in seismic velocity within the fields.

1.1 The Menengai prospect

Menengai-Olbanita area is located within a region of intracontinental crustal triple Rift junction. This is where the Kavirondo Rift joins the main Kenyan rift (Figure 1.1). The Kavirondo rift has been inactive since at least upper Pliocene. The main rift is bounded by N-S running major rift scarps that depict different tectonic style on the two sides. Bosworth et al (1986) proposes that this part of the rift represent a breakaway section of major lithospheric detachments as evidenced by sharp scarps in the eastern side and gentle sloping one on the western side. Geotermica Italiana Srl (1987) proposes that this whole section of the rift is a crustal detachment generating a sequence of faults, which merge at a low angle at depth. This is a situation described structurally as a 'reverse drag' where differential spreading is maximum on the master fault and rotation of faulted blocks result in tilted blocks. The central ring structures of Menengai and Olbanita calderas represent collapses associated with emptying of shallow magma chambers underlying them. Menengai-Olbanita area is located within a region that is considered to overly a mantle plume (Burke & Dewey, 1973). The surface is comprised of several eruptive volcanoes with caldera collapses and concentration of tectonic grid faulting (block and fissure faults) in its northern reaches which are characteristic of extension faulting associated with spreading (rifting) at crustal boundaries. On the surface, the area comprises widespread pyroclastics cover from the large caldera and it is also characterised by heavy masking by Menengai eruptives. Grid faults expose older lava to the north, mainly trachytic and trachyphonolites belonging to the 'Hannington suite (McCall, 1967).

The composition of the lava-flows found in the area varies from phonolites, trachyphonolites and trachytes. Subordinate alkali olivine basalts also occur in the area. Phonolites and trachyphonolites form the older lava eruption in the Rift floor and are more exposed in the northern parts. Most of the Menengai pre-caldera shields building lavas are trachytic. Similarly the post caldera lava partially filing the caldera floor is also trachytic.

Huge amounts of pyroclastics cover the slopes of Menengai and areas around Olbanita. These vary from ash fall, pumice rich ash deposits, welded pyroclastic flows (Ignimbrites) and some proximal lithic tuff outcrops adjacent to Menengai explosive caldera. The source of the pyroclastic eruptives is obviously the explosive eruption accompanying formation of Menengai caldera.

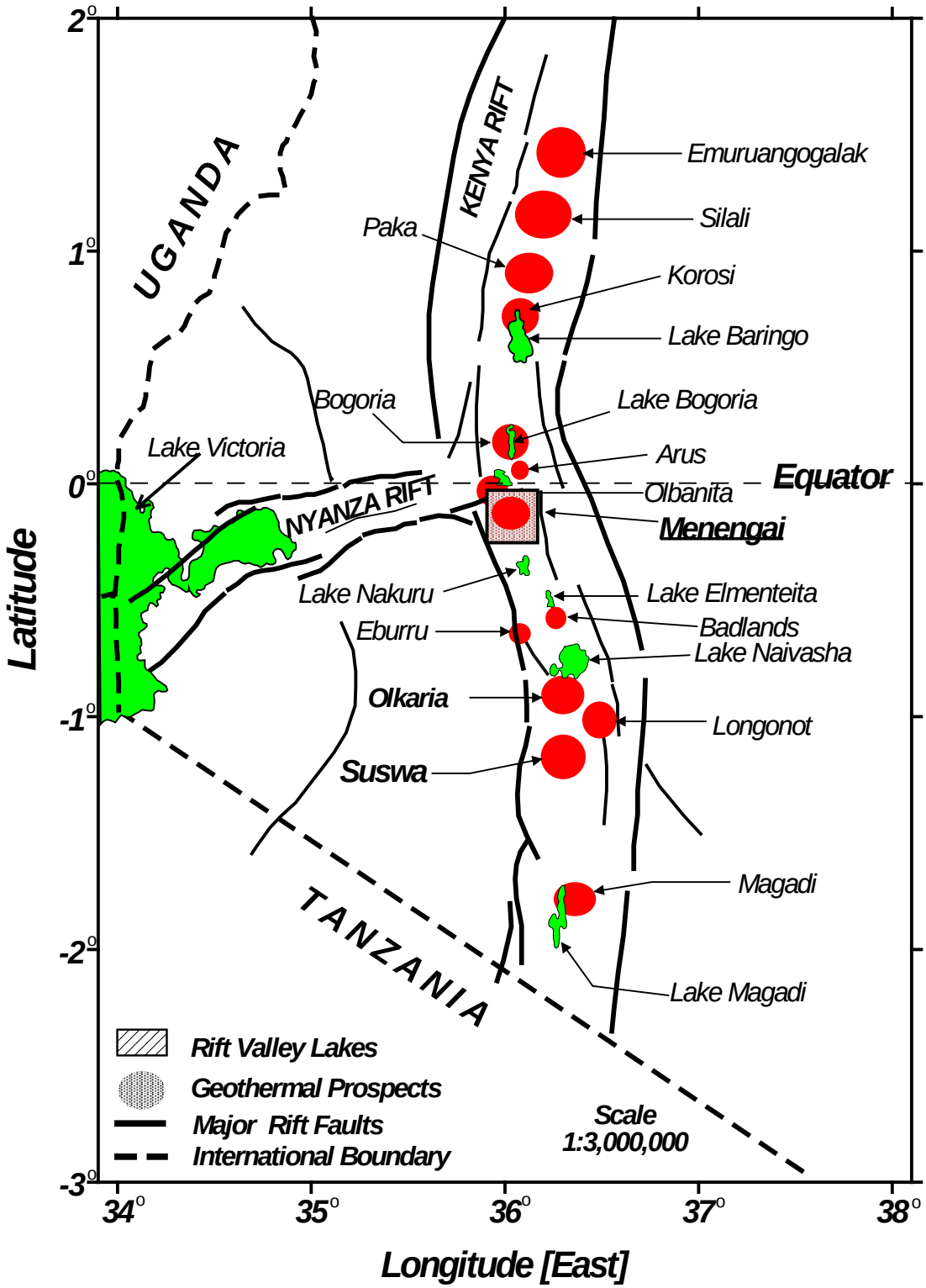

Figure 1.1. Map of the Kenya rift showing Lakes and Geothermal Prospects. The Menengai geothermal prospect is shown in a shaded box.

2. METHODOLOGY

Regional seismic refraction studies are normally carried out to identify areas with high seismic velocities that form targets for further detailed micro-seismic studies. For example, along the Kenya Rift, regional seismic studies of the crust (Henry et al., 1990; Mechie et al., 1994 and Mechie et al., 1997 and Simiyu and Keller, 2001) showed that there were significant differences in crust structure between the northern, Central and southern parts of the rift valley. The rift fill thickness varies from 1.5 km to 5 km underlain by basement material of velocity 6.05 km/s. They mapped high velocity bodies associated with the Menengai, Olkaria and Suswa Quaternary volcanic centres.

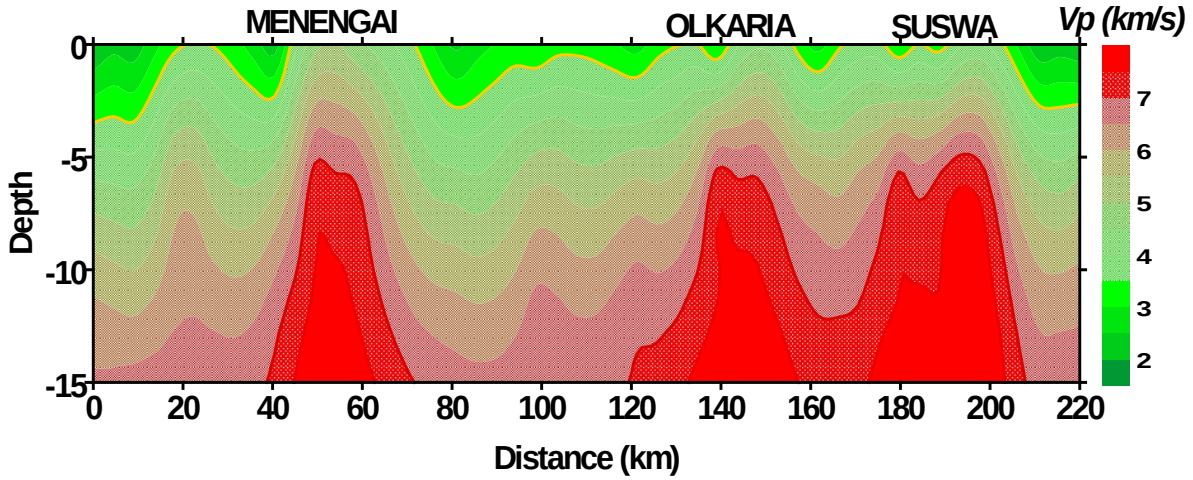

Figure 1.2. Seismic Velocity model along the Rift axis showing high velocity zones beneath Menengai, Olkaria and Suswa Volcanic centers based on the KRISP 1985-1990 axial model by Simiyu and Keller, 2000.

2.1 Data acquisition

2.1.1 Background noise monitoring

It has long been recognised that hydrothermal processes such as phase change within a geothermal reservoir radiate seismic energy (Whiteford, 1975). High levels of ground noise has been detected at many geothermal sites and some evidence presented for existence of radiating sources at some depth, e.g. Long valley, California (Iyer and Hitchcock, 1976) and Grass valley, Nevada (Liew and McEvilly, 1979).

Background noise is recorded in the fields as a function of time over 24 hours where the instruments are programmed with a 5 seconds recording window that triggers every 30 minutes in order to monitor the variation of ground velocity amplitude. The root mean square (RMS) of the ground velocity (Amplitude) is then calculated over the 5 sec window in microns/sec. For example at Menengai, the noise levels oscillated around a mean as shown in representative plots of the RMS as a function of time (Figure 2.1). The Menengai South West (MSW), Menengai South East (MSE), Menengai North East (MNE), Menengai Caldera Area (MCA), Menengai North West (MNW) and Menengai North Area (MNA) area have mean values of 2.5, 2.1, 1.5, 2.1,1.5 and 0.5 respectively.

An interpretation of the amplitude of ground velocity showed the value is highest in the MSW and MSE areas due to perturbation by cultural noise from the Nakuru town activity and traffic along the Nairobi-Nakuru-Eldoret highway. The MNE area shows very low noise levels during the night but

increases to the same levels as the MSW around mid-day when there is a lot of movement along the roads and town.

The MCA area has high mean noise level with a very large standard deviation mainly due to possible geothermal activities. The MCA has very limited cultural activities with the noise being mainly natural as opposed to the MSW and MSE. This is interpreted as possibly hydrothermal related radiating sources (Simiyu, 2003).

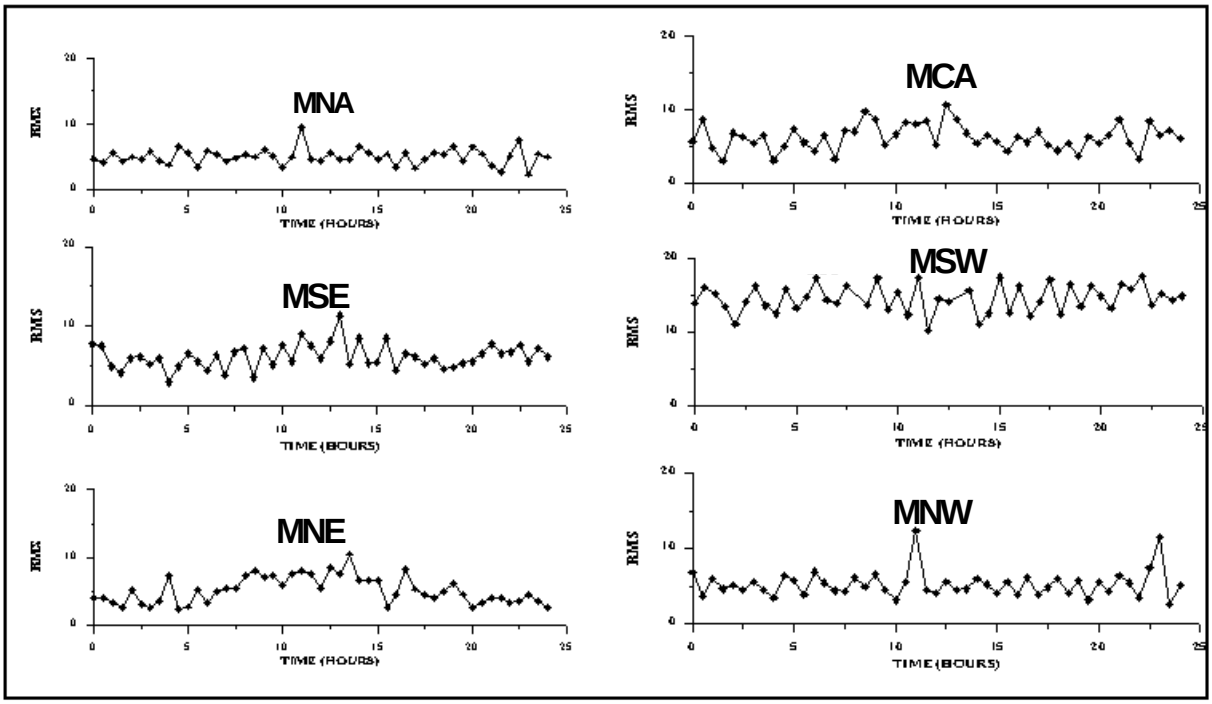

Figure 2.1. Background Seismic Noise in Menengai Area: MNA, MSE, MNE, MCA, MSW and MNW

2.1.2 Micro-seismic network

Months to years of continuous seismic monitoring using as many as 5 to 200 instruments are normally laid in a network to determine the locations and nature of the earthquakes within a given prospect area as shown in the Menengai Volcanic area (Figure 2.2). A wider area network can also be deployed centred on the main prospect of interest with raypaths expected to cross the volcanic centres. The wider network is normally aimed to determine the variation in physical parameters that are associated with the heat sources, heat transfer and fluid flow.

The ideal seismograph network for the prospect is mainly comprised of stations with recorders equipped with three-component short period (1-2 Hz) sensors and digital GPS timing systems. Initially broadband sensors are deployed in a rectangle around the field within the wider area network with one instrument at the centre of the polygon. This earlier deployment has been used to assess the suitability of later methods used by analyzing for the instrument response, the source effect and site effects.

The main project network is designed to cover the potential geothermal area with instrument locations close enough to detect events of low magnitude. The network is typically designed to cover an area of about 20 km across centred on the main prospect. Thus, for shallow earthquakes (depth <5 km) the outer stations would record waves refracted through basement rocks and the inner stations would record direct waves travelling through the shallow layers.

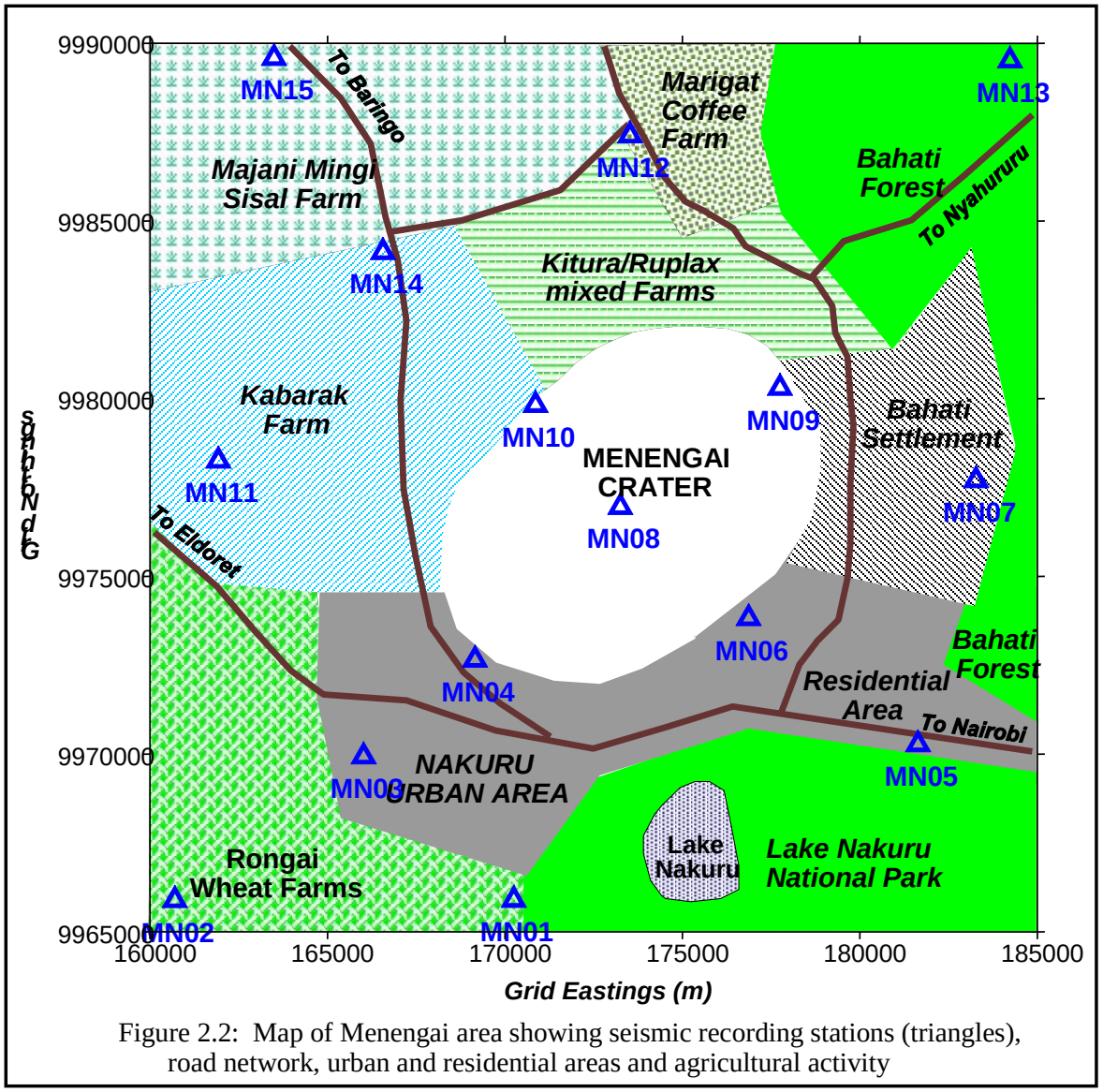

Figure 2.2: Map of Menengai area showing seismic recording stations (triangles), road network, urban and residential areas and agricultural activity

Seismometers are placed as close to outcropping rocks as possible in order to avoid noisy conditions and high attenuation associated with low velocity formations such as tuffs, soils and sediments. Pits are dug two to three meters deep for the seismometers through the loose cover to more consolidated material or base-rock where possible. A flat concrete base is then constructed with rock ballast and cement coupled onto the base-rock (country rock). For micro-seismics, instruments are programmed to sample at a rate of 250-500 samples per second on a data stream that can also be on trigger mode. A second data stream can be used at a different sample rate such as 50 samples per second but on a continuous recording mode. This second stream acts as security if there was a trigger parameter error. Also analogue recording instruments can be deployed alongside the digital ones to look at how the recording was going.

2.2 Data processing

2.2.1 Data picking

Data is downloaded directly onto a PC and processed using programmes such as PCSUDS and PITSA packages (Sherbaum and Johnson, 1994) where they are picked for the arrival times. When a P or S

arrival time is picked, the operator assigned that 'pick' a quality between 0 (good, error < 0.015 sec) and 3 (poor, large error-0.05 sec). This relative waiting of picks is included as a contributor to the earthquake arrival time error given as;

$$\varepsilon_r = [\alpha^2+\beta^2]^{0.5} \quad (1)$$

where, ε_r = Reading/Arrival time error;
α = Picking error; and
β = Instrument timing error.

2.2.2 Elevation corrections

The event location program assumes that recording stations are situated on a horizontal surface above a plane layered velocity model. To correct for this, a time delay based on the determined velocity of the shallow material within the topographic difference of the survey area was specified for each station and these were added to each set of arrival times. The reference levels are taken as the lowest station elevation within the survey area. Assuming near vertical incidence angles, the height difference between each station and the reference level is the travel path difference that is to be taken into account. To convert the height differences to time delays, the height was divided by the velocity of the material that makes the topography above the datum. The velocity defined for the top layer depended on the geology at the station. The elevation reference levels, maximum thickness and a determined velocity for the material above datum have to be determined and used for correction at each station.

2.2.3 Magnitude and event location

There are many packages used for event location and magnitude determinations. However, most of them are based on the HYPO71 package (Lee and Lahr, 1975). The P and S arrival times read from the sections are entered manually into the HYPO71 (or hypoinverse) for preliminary epicentre and hypocenter location. The data are analyzed, events identified and then located. In a new area a 1 dimensional P-wave velocity model is initially made for the whole area consisting of a number of flat homogeneous layers the bottom of which is a half space and used to give an initial location of events. In Kenya, for example, the initial velocity models of the rift volcanic areas are based on regional seismic refraction data and used in the event location.

The resultant model is tested with well-located events and finally modified to make the observed and calculated velocities agree. The model was then used to get the initial /preliminary event locations for the area.

The next step is to make a combined P and S wave crustal velocity model for the whole area. This can be made consisting of flat homogeneous layers with vertical linear velocity gradient. The program used can also allow for horizontal velocity changes in the BLOCK DATA subprogram. In order to refine the event locations by using both P and S waves, it is necessary to develop a velocity model that incorporates both P and S wave velocity. First, an average Vp/Vs ratio for the whole area is estimated using Wadati plots. Earthquakes with an arrival time pick of quality 0 and 1 are used and to avoid bias towards the more active zones, the earthquakes chosen should be evenly distributed throughout the area. Plots of travel time versus distance are constructed and the average velocities for P and S-waves obtained by linear least squares fit (with focal depth consideration in the epicentre distance calculation). The determined Vp is then divided by Vs to obtain the ratio.

To cross check the results, S-wave travel times are plotted against P-wave travel times for a number of earthquakes and the slope of a linear least squares fit gives the same the Vp/Vs ratio. These two

approaches should give comparable results. In most cases, the earliest S-arrival time is picked; hence the results of the analysis are in most cases biased towards the faster S-wave velocity. The new model combining P and S-waves is then used to relocate the events and then compared with the initial locations using a P only velocity model.

Using a combined P-wave and S-wave velocity model instead of the P-wave velocity model alone can reduce the location errors by 12-23 % horizontal and 13-28 % vertical. Normally the errors are lowest for those events from the centre of the network and highest for the events outside. A typical velocity model for Olkaria, Kenya (Simiyu 2000) is given below.

Layer	Depth [km]	V_p [km/s]	V_s [km/s]	Lithology
1	0 to 0.6	2.1	1.2	Pyroclastics
2	0.6 to 2.5	3.3	1.9	Trachytes/Tuffs
3	2.5 to 3.5	4.5	2.6	Lavas/Intrusives
4	3.5 to 4.5	5.2	3.1	U. granitic basement
5	4.5 to 8.0	6.4	3.8	L. granitic basement

The events are located and then classified according to arrival time differences into a number of categories such as an example below:

1) Local events [T_s-T_p<5 sec];
2) Regional events [5<T_s-T_p<40 sec];
3) Tele-seismic events [T_s-T_p>40 sec].

Commonly used is the formula given by Lee et. al. (1972) to evaluate the duration [coda] magnitudes.

$$M_c = 2\log[C] + 0.00325d - 0.97 \quad (2)$$

where, d = epicentre distance [km]; and
C = duration of the earthquake coda [seconds].

The magnitudes of the earthquakes mostly recorded in geothermal areas are normally between M_c=1.5 and M_c=3.0.

Many studies in geothermal fields have shown that the velocity structure at most of the volcanic centres is heterogeneous from the surface up to 4 km. One velocity model that does not allow for lateral velocity variation is therefore not adequate for precisely locating earthquakes that span 2 of the regions. To reduce the problem of heterogeneity in such a case, each event can be located using the velocity model of the region of origin and stations within the region. Those stations close to the event are given more weight. During back projection, a laterally homogeneous velocity is assumed. The strong lateral variation in the upper zones (1-4 km depth) will not significantly affect the back projection if the rays used have hypocenters deeper than for example 4 km. Heterogeneity due to local anomalies may affect the ray paths more significantly such as lateral refractions around anomalously slow regions, which will produce a smaller image of the anomaly.

The next step in this approach is to break down the data into smaller hypocentre-station groups consisting of earthquakes originating from one part of the field (belonging to the same swarm). It has been found in many fields that the seismicity patterns varied from one area of the field to another. Such a field can thus be divided into a number of areas. It has been found in many areas that the scatter greatly reduces with a standard deviation of 0.011 to 0.04.

2.2.4 Error analysis

The analysis program calculates the full 4x4-covariance matrix of the solution, and derives from it the error ellipsoid and the horizontal and vertical errors. The error calculation requires an estimate of the variance in the arrival time data, given as;

$$\omega^2 = \varepsilon_r^2 + \varepsilon_f * rms^2 \quad (3)$$

where, ω^2 = variance (standard error squared) of the arrival time data;
ε_r^2 = estimated reading error; and
ε_f = weighting factor for including the effect of a poor solution.

The mean location errors calculated by HYPO71 using the combined P and S wave velocity model for the different fields in Kenya is on average typically; horizontal error of 0.3 km and a vertical error of 0.6 km.

2.3 Determination of detailed V_p/V_s ratio variations

Two typical detailed Vp/Vs ratio determination methods as applied for the Menengai area of Kenya is discussed next.

2.3.1 Using Wadati plots

The approach is to break down the data into smaller hypocenter-station blocks of 1x1 km. These blocks are made such that they are consisting of events originating from the same block of the field (belonging to the same group or clusters that are less than 1 km apart). The Vp/Vs values are then determined for each divided block using the Wadati plots. The Wadati plot is a statistical method that is based on least squares fit approach.
The approach to this velocity ratios analysis for the Menengai prospect area was to determine;

1) an average overall V_p/V_s ratio for the whole of the Menengai area to use in Hypo71; and
2) Spatial variation of the measured V_p/V_s ratio throughout the study area.

1567 well located earthquakes each with an arrival time pick of quality 0 and 1 were used. To avoid bias towards the more active zones, the earthquakes chosen were evenly distributed throughout the area. Simple plots of P and S wave travel time versus distance for the same data set were constructed and the average velocities for P and S waves obtained by linear least-squares fit (with focal depth consideration in epicentre distance calculation). This was important as some of the events originated in areas localized velocity anomalies.

The determined Vp was then divided by Vs to obtain the ratio. To cross check the results, S arrival times were plotted against P arrival times for a number of earthquakes and the slope of a linear least squares fit gave the Vp/Vs ratio. It was found that these two approaches gave comparable results. In all cases, the earliest S-arrival time was picked hence the results of the analysis are probably biased towards the faster S-wave velocity. These plots for the whole area show very pronounced scatters. On the basis of these ratios, velocity models were developed for both the Olbanita area and Menengai caldera areas. (Figure 2.4a and 2.4b).

The highest Vp/Vs ratios were mainly for earthquakes outside the network and most of them were for earthquakes with an NE azimuth. Figure 2.5 shows the average distribution map of Vp/Vs ratios within the whole of Menengai area. This map shows that the caldera centre, north eastern caldera rim and the Olbanita area have the lowest average ratios. The MSW, MSE, MNE and other areas outside the caldera and Olbanita have the highest ratios.

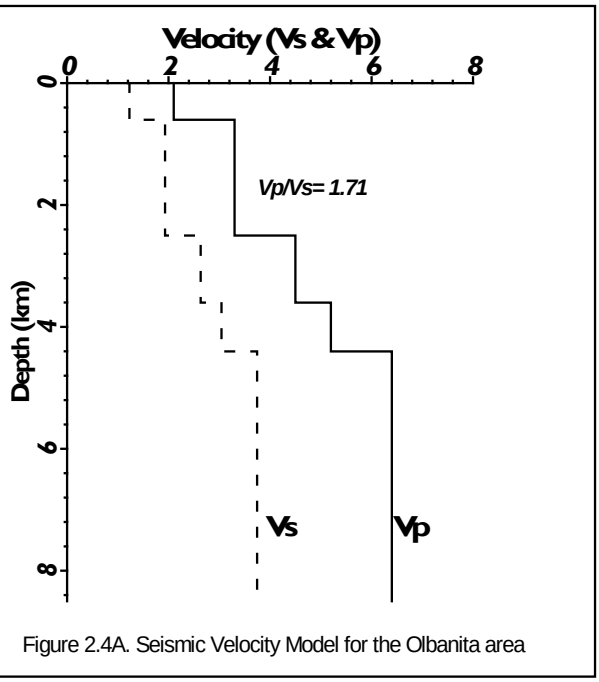

Figure 2.4A. Seismic Velocity Model for the Olbanita area

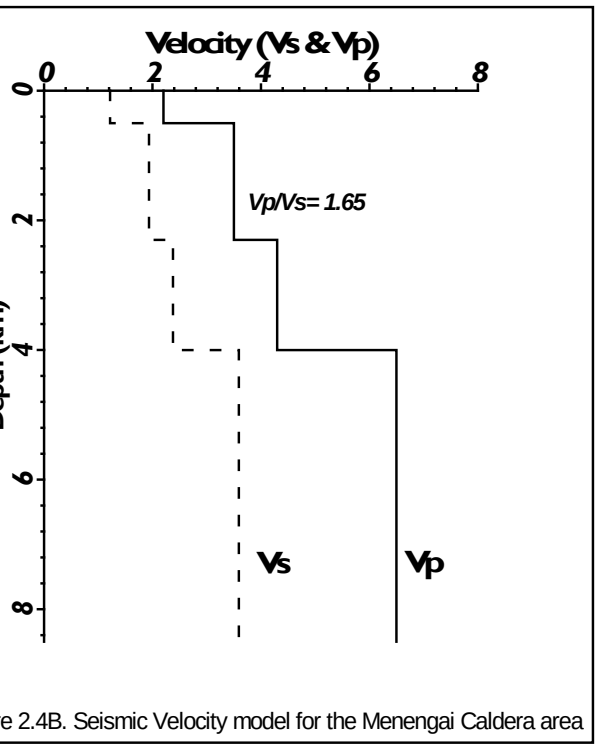

Figure 2.4B. Seismic Velocity model for the Menengai Caldera area

2.3.2 Direct V_p/V_s inversion method

The arrival times were inverted using the computer program SIMULPS12 (Evans et al., 1994). This program is a modification of the original code by Thurber (1994) that uses raytracing. The modified program that we used solves simultaneously for earthquake locations and the crust structure (Vp and Vp/Vs) by the iterative damped-least squares method. At each iteration step, ray paths and earthquake locations are fully updated. The starting model was a 1D model determined earlier and used as a starting point for the inversion. The initial determined Vp/Vs ratio of 1.71 was used.

3D models were derived in a series of inversions in which starting with an initial course grid 100 notes at 5 km spacing. This was made progressively finer and the final grid has 1400 nodes and 0.5 km spacing with a final model giving RMS residuals of 0.03s P waves and 0.067s for S waves.

A resolution evaluation can carried out using the standard methods discussed by Foulger et al., (1995) by dividing the geothermal prospect area into blocks. The analysis results showed that the areas around the centre of the field are well resolved to a depth of 4.5 km. The developed ratios and velocities are then used to relocate the events.

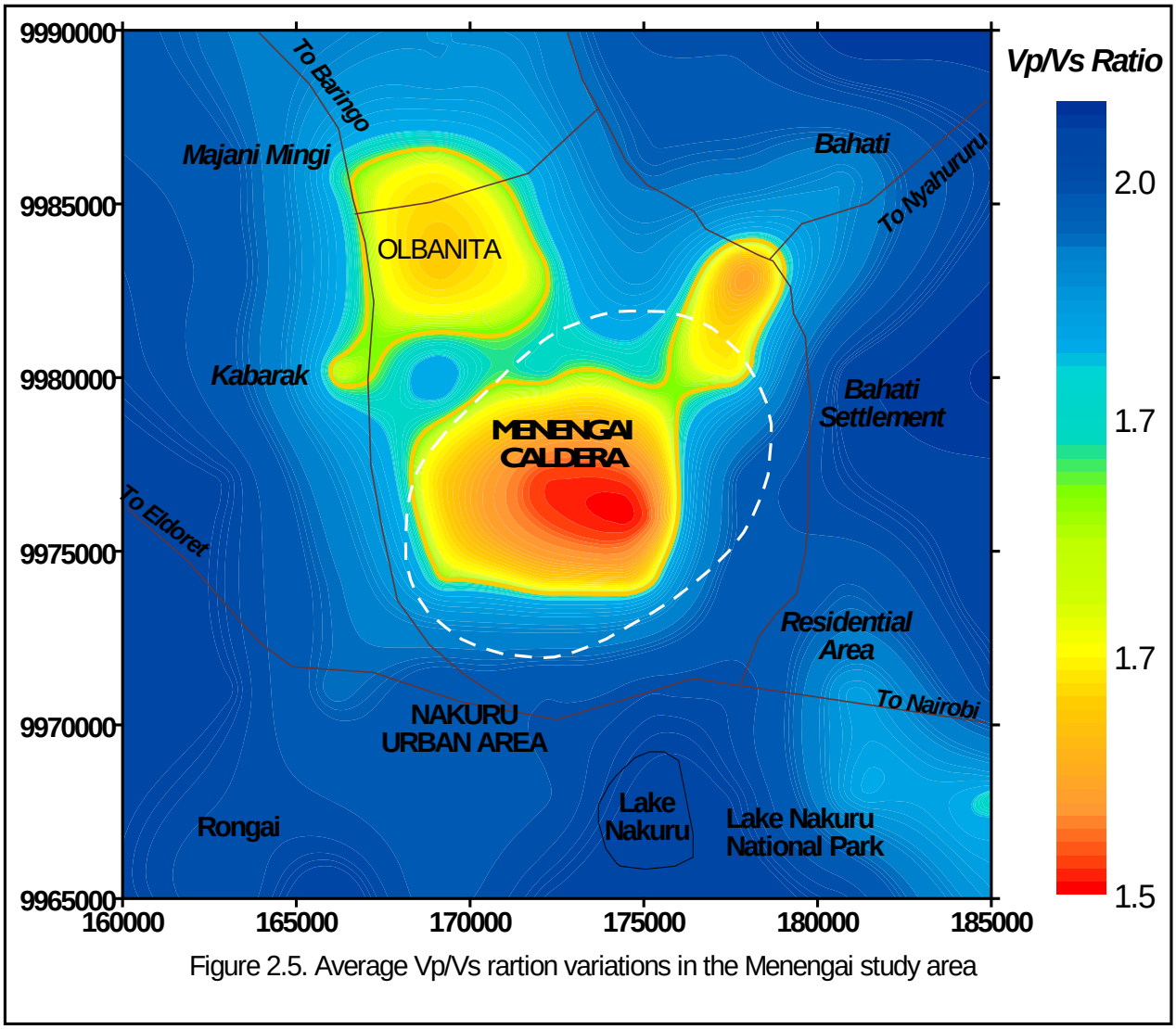

Figure 2.5. Average Vp/Vs rartion variations in the Menengai study area

3. RESULTS

3.1 Event distribution and magnitude variations

Figure 3.1a show the distribution of seismic events located within the Menengai prospect. Events are more concentrated within the Menengai caldera. This is the area around the central to the southern part of the caldera and on the NE caldera wall. Another area with a large cluster of events is within the Olbanita area to the central NW of the Menengai caldera where the events are also shallow (Figure 3.1b). The dashed line represents a zone just above the brittle ductile transition. At a larger scale, the events occur along two trends. The first trend is along the rift axis in a NNW-SSE trend that starts from Majani Mingi through Olbanita, Menengai and dies out at Lake Nakuru in the South East. The second trend is parallel to the Nyanza rift axis in NE-SW direction along the major axis of the caldera with clusters from Bahati on the Aberdare ranges, through the caldera, Nakuru town and Rongai.

The Menengai caldera appears to be at an intersection of these two trends and thus at a triple junction. This shows that these fault zones along the rift axis and Nyanza Rift are still active and their point of intersection is therefore likely zones of magma injection and thermal fluid up-flow.

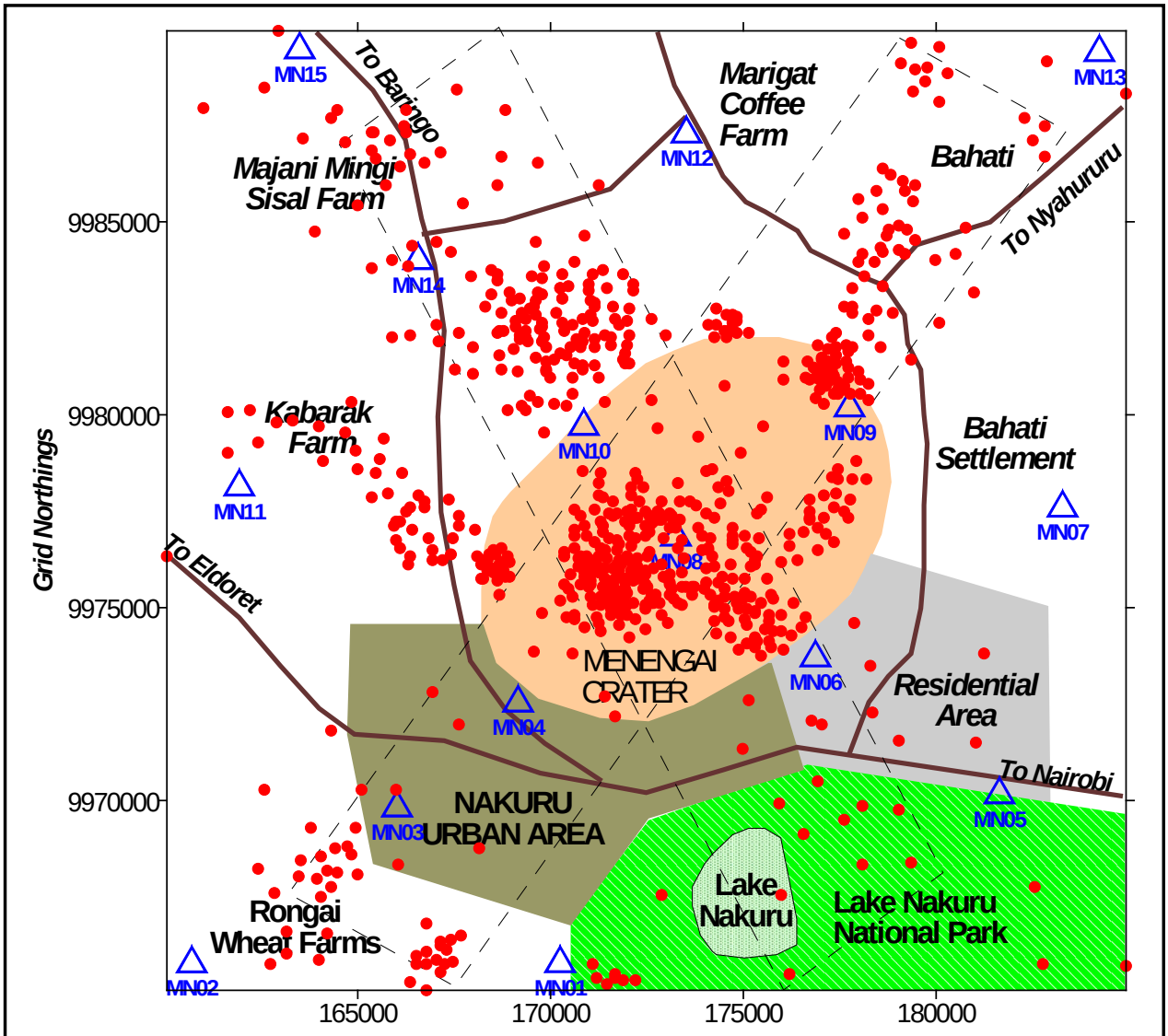

Figure 3.1A. Map showing recording stations [Triangles] and epicentres [circles]

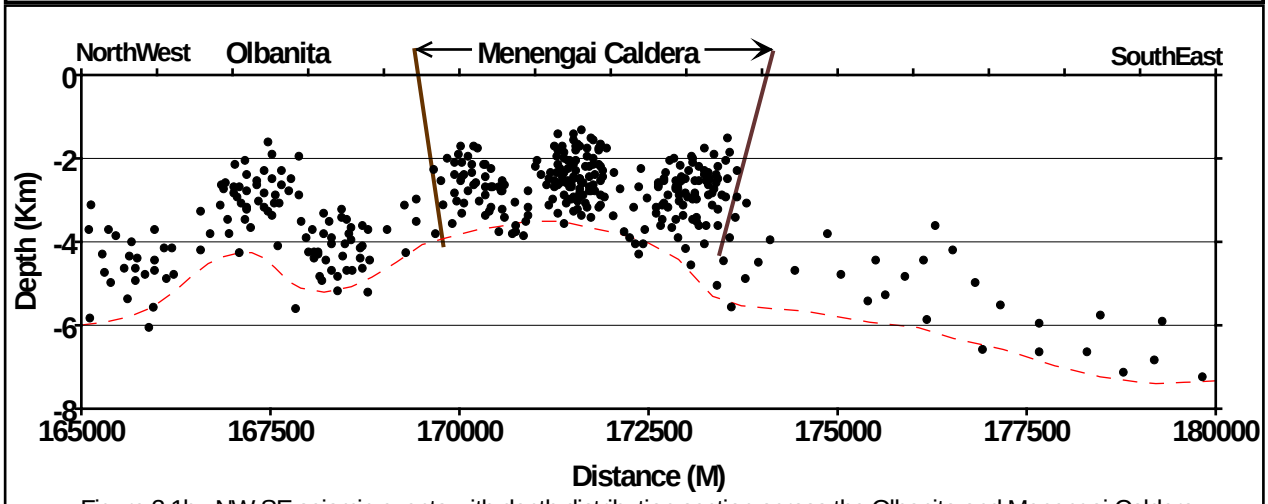

Figure 3.1b. NW-SE seismic events with depth distribution section across the Olbanita and Menengai Caldera

At Menengai, an averaged seismic distribution with depth map (Figure 3.2) shows that the area to the SW, SE, E and W are thermally under-privileged as the seismic cloud density decreases with depth. Around Olbanita and Menengai caldera, the events are smaller and shallower and deepen away from the caldera towards the SE, NW, North, West and East. The plots show a central area with intense seismic activity with shallow events centred on the Menengai caldera. It is therefore reasonable to assume that this zone of shallow events represent an area overlying the heat source for the geothermal system.

Magnitude-distance distribution for earthquakes located within the array (the prospect area) show that a greater proportion of the smallest earthquakes of magnitude 1.5 and less are recorded very close and within the network centre but fewer and larger magnitude 1.5 and greater on the periphery. This result is similar to recording in other high temperature and pressure geothermal fields such as Olkaria, Kenya (Simiyu and Malin, 2000), Mammoth (Stroujkova and Malin, 2000) and Geysers, USA (Combs, 1984).

In the absence of any specific magnitude formula determined for the southern part of the Kenya rift, we used the formula given by Lee et. al., (1973) to evaluate the duration magnitudes.

$$M_c = 2\log[C] + 0.00325d - 0.97 \quad (4)$$

where, d = epicentre distance [km]; and
C = duration of the earthquake coda [seconds].

The magnitudes of local earthquakes show that there are no duration magnitudes for local earthquakes higher than 2.7 within the network, but magnitudes around 0.5-1.5 are regularly occurring. Figure 3.3 show the magnitude-distance distribution for earthquakes located within the array. This figure shows that a greater proportion of smallest earthquakes are recorded very close and within the network centre but fewer and larger magnitude earthquakes away from the network.

3.2. Heat source mapping

Although a number of studies have been carried out in the Menengai Geothermal Area, there has been no attempt to determine the presence and status of magma heat sources. A model relating the heat sources to the observed geophysical anomalies, volcanic evolution, reservoir characteristics and resource potential has not been developed.

3.2.1 The brittle-ductile transition zone

Under normal conditions, there is a linear increase in the crust strength with pressure (depth) and exponential decrease in strength with temperature. Peak strength is expected at a transition point from the brittle (pressure controlled) zone called the seismogenic zone to the ductile (temperature controlled) zone (Kohlstedt et al., 1995). The amplitude and depth of the seismic activity peak is predicted to decrease with increasing geothermal gradient. Earthquakes represent a sudden slippage of rock along a fracture surface and generally should be restricted to a zone of brittle deformation. The maximum depth in a region at which earthquake intensity peaks will delineate the brittle-ductile transition zone (Meissner and Strehlau, 1982).

Chen and Molnar (1981) showed that temperature is a dominant factor in determining the maximum depth of earthquakes. Temperatures of less than 450^o C are required for an earthquake to occur in the crust rocks. At Menengai, the seismic activity depth relationship (Figure 3.2, 3.3 and 3.4) shows that the area within the caldera and Olbanita area is thermally privileged as the seismic cloud decreases with depth. Around these areas, the events are smaller and shallower and deepen away from the caldera towards the East, West and South. A contour map of averaged event depths shows a NE-SW

trend of the area with intense seismic activity with shallow hypocenters centred on the caldera. Another NNW-SSE trend through Olbanita is centred on the SE caldera edge. It is therefore reasonable to assume that these zones of shallow events within the two trends actually represent the areas overlying the heat sources for the geothermal system.

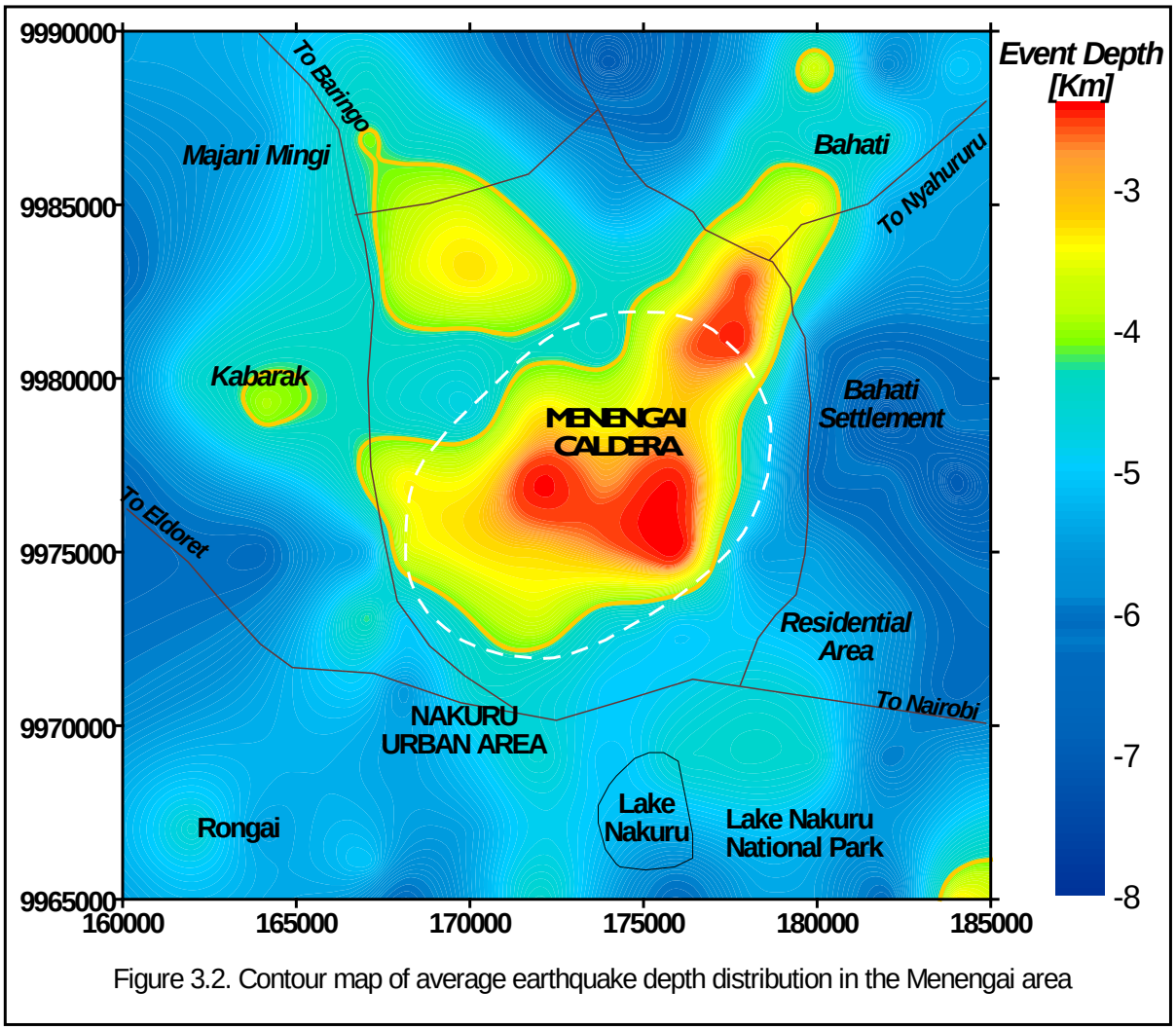

Figure 3.2. Contour map of average earthquake depth distribution in the Menengai area

Heat flow measurements in this area of the Kenya Rift (Wheildon et al., 1994) showed very high heat values (about 200 MWm^{-2}). In this area a change in seismic intensity at a depth of 5-7 km represent the brittle-ductile transition zone within the network. This depth is reasonable given the high geothermal gradient with temperatures of up to 340^{o} C measured in wells at a depth of 2 km.

These results are consistent with detailed analysis of gravity data (Simiyu and Keller, 1998) which show a positive anomaly with an amplitude of 30 mGal, half-wavelength of 15 km and a NW-SE trending anomaly interpreted to be related to the heat source. Band pass filtering indicated that the NE-SW trending anomaly has two maxima with amplitude up to 15 and 24 mGal. They also identified linear positive anomalies showing control of structures in the basement and shallow bodies related to Menengai volcanic activity. During this study, a basaltic melt magma body was postulated as the main heat source directly beneath the caldera.

All these data sets show that there exists a shallow high temperature body located directly beneath the caldera. This body is the likely heat source for the geothermal system. The distribution of epicentres in Menengai show more intense, smaller and shallower events are prominent in the centre of the field and

larger, deeper events on the periphery. 95 % of the events recorded having magnitudes less than M_c=2. This implies that the centre of the geothermal system is in a low stress state because stress is being released at a different rate to the surrounding areas with the rift flanks having the highest stress levels.

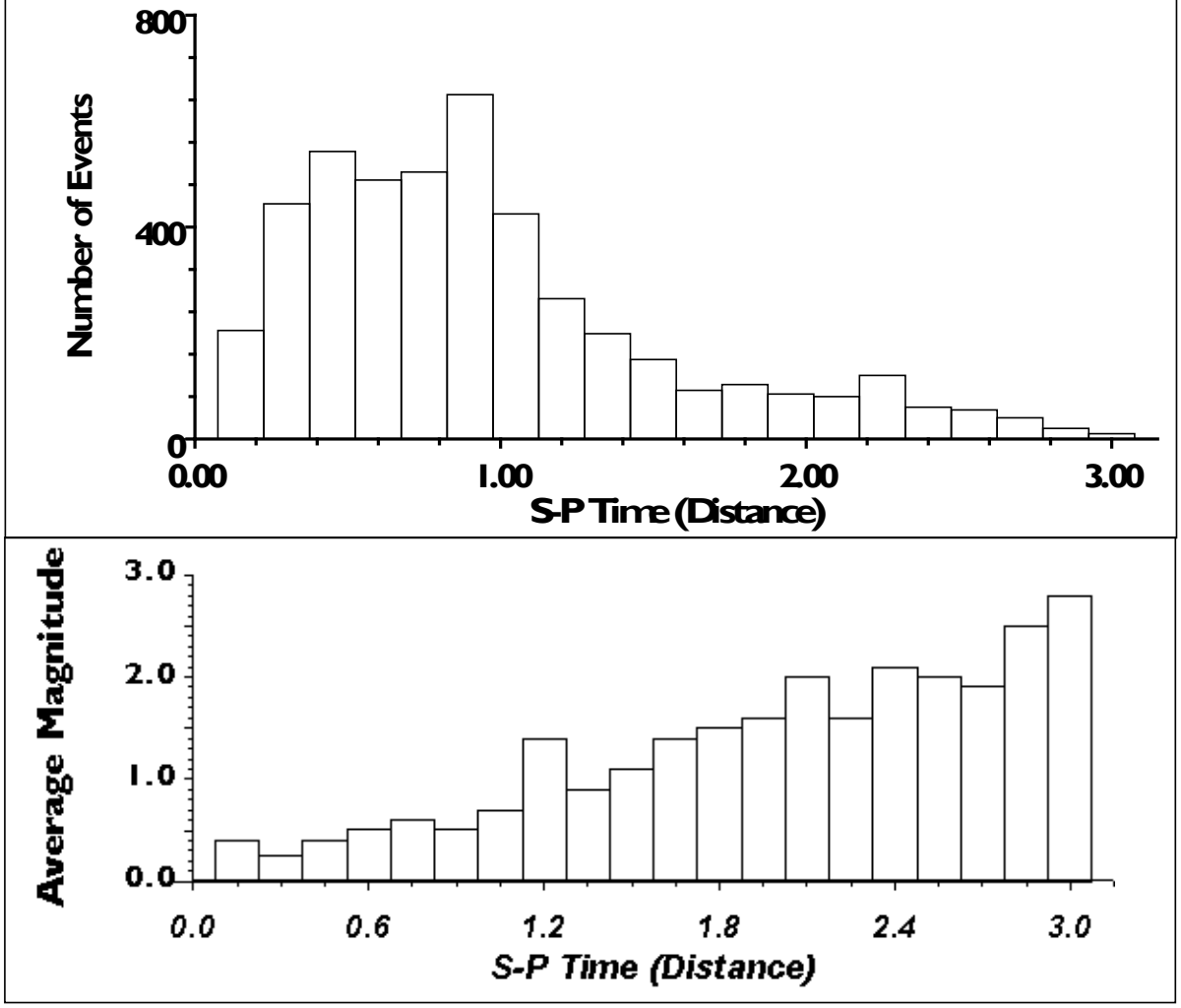

Figure 3.3. Plot of Frequency Vs Distance and Magnitude Vs Distance distribution from the center of the field for recorded events.

This implies that event depth is related to subsurface temperature and hot fluid flow patterns. Depth distribution may also be a reflection of the variation in the brittle-ductile transition depth within the study area as suggested by Meissner and Strehlau (1982) and Simiyu and Malin (2000). It seems reasonable to assume that the earthquake cut-off depth of 7 km (Figure 3.4) actually represents the start of the ductile zone. This depth is very important for determining the depth to the heat source, which is expected to be at a depth of about 7 km. outside the network, earthquakes deepen to the Southwest, South and Southeast away from the centre implying a deeper brittle-ductile transition zone.

Fairhead and Stuarts (1982) suggest that stress along the rift floor in the Central Kenya Rift (CKR) area is being released by micro-seismic activities in geothermal areas but by larger earthquake sequences along the rift boundary faults. This interpretation is also supported by recent seismic intensity, magnitude and depth distribution analysis in Lake Bogoria and Olkaria by Young et al. (1994) and Simiyu (1999). Their results indicate that seismic activity is more intense in the centre of

the volcanic fields (rift axis) where temperature is high, with smaller and shallower events that become larger and deeper on the periphery (rift flanks).

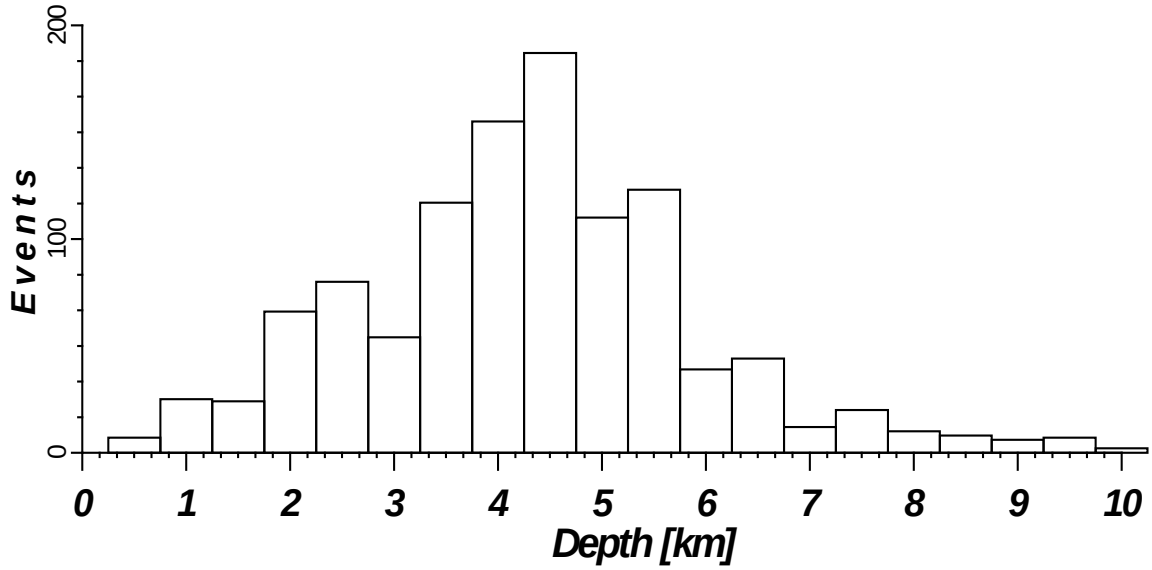

Figure 3.4A. Histogram of earthquake frequency distribution with depth

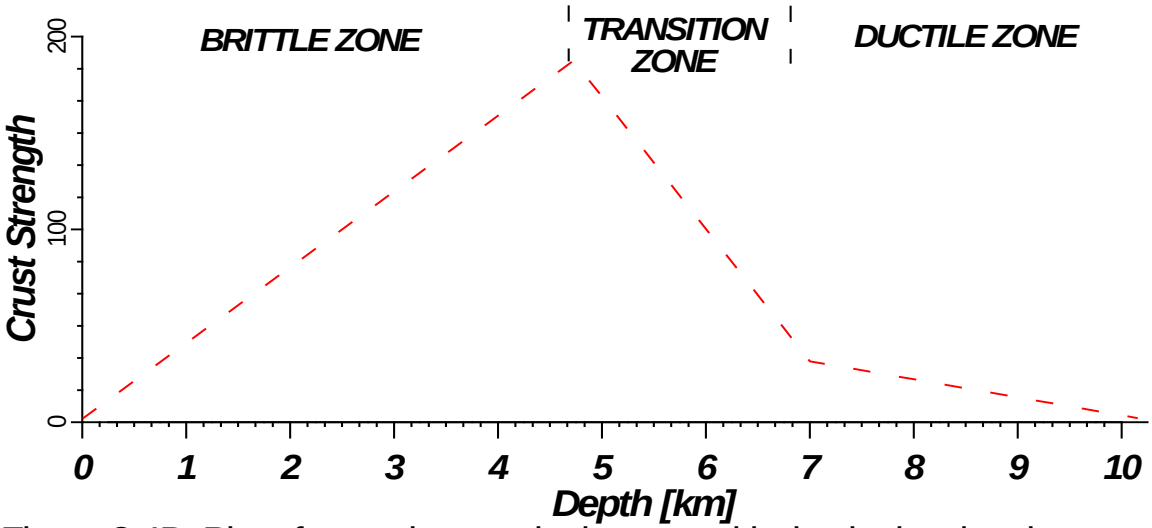

Figure 3.4B. Plot of crustal strength changes with depth showing the Brittle, Brittle-Ductile transition, Ductile Zone

3.2.2 Shear wave attenuation studies

Geothermal fields owe their existence to the presence of molten rock in the crust. The location of these bodies in many fields has been mapped by analyzing regions of high S_v wave attenuation (Sanders, 1984; Ryall and Ryall, 1981; Matumoto, 1971 and Einarsson, 1978).

During routine analysis of seismograms for arrival times and first motion (Simiyu et al., 1998), it was realized that some of the seismograms had diminished S_v wave amplitudes. Spectral analysis showed that the signals were of low dominant frequencies (less than 3 Hz). This was taken to imply that the rays were passing through a molten body or less compacted low velocity material near surface. It was

therefore necessary to determine the real cause of the low dominant frequency whether it is a source, transmission, instrument or site effect.

There has been continuous monitoring during the last nine months that has objectives to analyze earthquake distribution and properties across the geothermal area. The purpose of this was to evaluate the presence of S-wave attenuating bodies that could constitute heat sources for the geothermal systems. The seismic network shown in figure 1.3 was used to study the attenuation effects beneath the Menengai volcano and the areas surrounding the geothermal prospect.

3.2.3 Event selection

The network records an average of 26 events per day and during this study, we chose events with at least 4 station readings, rms residuals <0.09 sec, horizontal error <1.0 km and vertical error <1.5 km. To avoid bias towards the dense network clusters, the area was divided into blocks of 2 km2 and maximum 2 events taken from each block, thus reducing the total events used to 147. Initially 433 events were selected then we chose seismograms with arrival time pick quality 0 and 1 for amplitude analysis. Maximum peak-to-peak P and Sv wave amplitudes were measured within the range of their expected arrival times on the vertical component record.

Amplitude determinations were done before the events were located to avoid possible bias. 147 events that showed attenuation effects have been used in the final analysis and location of attenuating bodies. 25 of the 147 events shown in table 4.1 have been chosen and are used here to show the ray paths and surface projections of normal and attenuated signals. Figure 3.5 shows the raypaths of events within the study area and outside used to study the attenuation. The outlines of the attenuating bodies beneath Olbanita and within the caldera are projected on the surface in this figure.

The events were grouped according to a scheme that had been developed during this study. This scheme is based on the relative attenuation of the S_v waves and similar to the methods used in the Long Valley caldera by Sanders (1995) and at Yellowstone national park:

Type I	Severely attenuated S_v waves [S_v/A_p <0.4]. These are events whose ray paths have traversed attenuating bodies.
Type II	Moderately attenuated [0.4< S_v/A_p >0.8]
Type III	Slightly attenuated [0.8< S_v/A_p >1.2]
Type IV	Normal [S_v/A_p >1.2]. These are events whose ray paths have not crossed attenuating bodies

TABLE 3.1: The table is showing the seismic events used to map the location of bodies that cause the attenuation of waves. Also shown are the event location, hypocenter, magnitude, and date and origin time

Event	East	North	Hypo	Mag.	Date	Origin Time
01	172.0	9990.8	09	2.2	03/01/02	21 12 13.721
02	186.1	9978.7	11	2.4	20/05/02	18 23 11.817
03	191.8	9981.7	10	2.6	01/01/02	11 56 45.025
04	189.8	9981.8	08	2.2	13/04/02	02 31 05.312
05	173.4	9990.8	14	2.9	01/02/02	00 06 54.120
06	169.6	9992.2	15	2.6	26/05/02	17 51 32.314
07	172.0	9986.6	11	2.5	10/02/02	20 29 25.070
08	174.7	9981.1	12	2.1	23/03/02	12 05 43.201
09	185.8	9976.8	14	3.2	09/02/02	00 10 09.563
10	181.4	9961.9	09	2.5	08/03/02	16 43 08.774
11	192.1	9951.9	11	2.5	20/04/02	02 20 52.141
12	179.9	9960.0	13	2.2	12/03/02	23 21 33.992
13	174.7	9953.1	14	2.5	28/05/02	07.00 51.886
14	187.0	9963.9	17	2.3	27/01/02	09 52 12.864
15	191.2	9967.0	14	2.8	03/03/02	21 04 34.628
16	186.0	9969.0	17	2.3	13/01/02	13 59 55.332
17	184.5	9954.5	10	2.1	26/04/02	22 49 45.011
18	187.7	9987.0	11	2.3	10/03/02	01 55 23.346
19	185.7	9973.2	15	2.7	03/02/02	01 14 13.574
20	173.6	9969.9	13	2.6	11/03/02	02 43 39.642
21	191.4	9959.2	17	2.9	08/01/02	03 36 59.701
22	177. 9	9951.2	16	2.6	27/05/02	19 27 41.034
23	188.9	9952.8	12	2.7	19/02/02	16 11 22.736
24	192.9	9970.1	18	2.2	21/04/02	08 32 47.178
25	171.4	9970.1	16	2.2	02/05/02	03 25 18.004

3.2.4 Focal mechanism

Focal mechanisms were analyzed manually using patterns of the P-wave first motion for some of the events used in this study. The arrivals were plotted on equal area projections of the upper hemisphere using the take-off angle, polarities and azimuth calculated by hypo-inverse. In this case, only the best-located events with less than 1 km horizontal and 1.5 km vertical error were used. It was also ensured that the events used had clear P-arrival polarities. Seismograms from several events with well-constrained focal mechanisms were compared to test the possibility of source effects being the main causes of attenuation. In particular, two events that occurred at the same epicentre were used and showed that the low amplitudes recorded on some records is not due to source effect.

It is known that shear wave amplitudes may be related to the position of the recording stations relative to the pattern of S_v energy radiating from the earthquake source. Low amplitudes have therefore been in many studies measured near nodal planes. Events with constrained mechanisms are used to determine whether the low amplitudes recorded are due to the position on the S_v radiating pattern or propagation through attenuating bodies. It is therefore necessary to determine whether the attenuation of the S-wave energy could not be related to their positions on the nodal plane and not due to a high temperature related magma body.

The selective attenuation of shear waves indicates that some rays passed through a fluid, probably molten rock. The rays from some events were not as much affected along their travel path since the

origin depth is shallow and thus the seismograms would show normal amplitude. Postulated surface projection of all ray-paths for different event-station azimuth variations is shown in Figure 3.5.

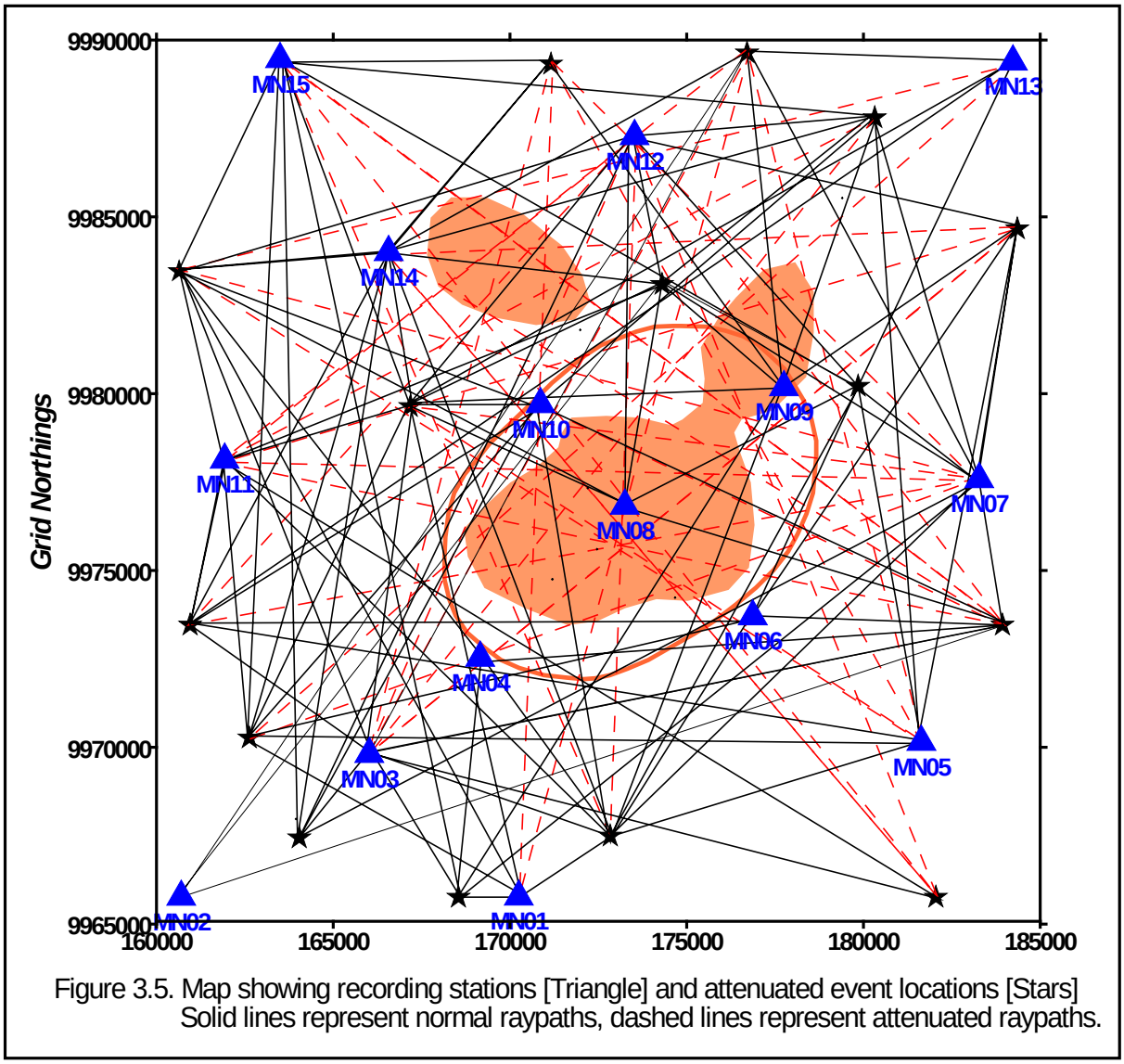

Figure 3.5. Map showing recording stations [Triangle] and attenuated event locations [Stars] Solid lines represent normal raypaths, dashed lines represent attenuated raypaths.

3.2.5 Spectral analysis

It has been shown in other studies (Aki et al., 1977) that the dominant frequency in hydrothermal and volcano-tectonic events if measured close to the source of origin could be related to the source effect and has nothing to do with propagation effects.

To determine the spectral content of events at Menengai required a great deal of attention. The recording was done such that the event to be analyzed must have been recorded close to the source of the signal to avoid mis-interpretation. It was found that events, which appear with low frequency content at a longer distance, are sometime high frequency events at the source. The higher frequencies are removed by attenuation during wave propagation through poorly compacted low velocity rocks. This was mainly evident for events with source that have near surface origin. However there were recorded deeper events that mostly originated from outside the volcanic area whose ray-paths crossed the area at a depth of more than 7 km. These events had also diminished S-wave amplitude.

During this study, the seismograms showed that a single event had different waveforms and a spectral content that varied from one record station to another depending on azimuth and take-off angle. The seismic signal records were divided into two groups.

I. Show high levels of S-wave attenuation characterized by a weak emergent phases for both the P and S-wave window followed by a phase of near uniform amplitude but at the same frequency. A strong dominant frequency is observed at 2-3 Hz.
II. This group involved seismograms that did not show any attenuation of the S-wave. They had clear P and S wave arrivals. The records have a relatively sharp onset of the signals with a wide range of frequencies. A mixture of dominant and sub-dominant frequencies varied from 2.5 Hz, 3.2 Hz, 3.5 Hz, 5.5 Hz and 8.6 Hz.

3.2.6 Attenuating sources

Geologists have over the years argued for the presence of highly evolved material beneath the Menengai volcanic field. Results from the present study show that there is no evidence for attenuating bodies to a depth of less than 6 km throughout the entire area. All the attenuating signatures come from events that have traversed the area deeper than 6 km. The attenuating bodies could not be fractured rocks saturated with hydrothermal fluids because:

I. It would have been detected throughout the entire circulation system from near surface down to the heat source.
II. It would have had a concave upward shape. The shape of attenuating bodies is concaving downwards consistent with the shape of a magma body.
III. Attenuation would have decreased with depth due to fracture sealing as a result of hydrostatic pressure.

Studies in Olkaria (Simiyu et al., 1998) show that complete sealing of fractures in this area occurs by 4-5 km depth. The picture we therefore get is that of off-shots of magma bodies coming off a main deeper body and penetrating the crust to shallow levels.

3.2.7 Olbanita area magma

The magma body is situated in the Menengai west area directly beneath Menengai volcanic centre. Figure 3.5 show normal and anomalous ray-paths beneath the Menengai caldera and Olbanita area to different stations spread within the area. Analysis of ray-paths through the Olbanita area anomaly shows that the boundary is constrained to the south by rays from the western area to station MN09, MN07 and MN13. The northern boundary is also well constrained by rays to station MN11, MN12 and MN15.

The western boundary is also well constrained. NS ray-path sections through the Menengai caldera show anomalous records at station MN04, MN15 and MN03. Depth to the top of the body is constrained at about 7 km. The Olbanita body peaks directly beneath the area of the postulated buried Olbanita caldera (Mungania, 1999).

3.2.8 Menengai caldera body

Distant events recorded at stations were picked at large spacing intervals in the whole area across the rift stretching from the two rift flanks on the Aberdare range and the Mau escarpment. These stations have been used to monitor deep events from both sides of the rift flanks with ray-paths that seem to have crossed the rift floor within the Menengai geothermal area. These events have been used to determine the nature of the root of the seismic attenuating bodies beneath the Menengai caldera.

Rays that are projected to have passed beneath the volcanic field at a deeper level have been used to map the magma root. The boundary of the attenuating body is well constrained to the north by deep attenuated and normal ray paths recorded at stations MN11 and MN07 for events from the two adjacent rift flanks. Ray paths recordings at station MN11, MN04, MN06, MN05 and MN07 were used to define the southern boundary. The ray-paths and section show that there is possibly a single deep body that is feeding the shallow magma centres at both Menengai and Olbanita.

Some raypaths north of the caldera and Olbanita area also show some limited effects of attenuation. The presence of these attenuated rays outside the caldera shows that there is a possibility that there could be other attenuating sources outside the caldera structure to the north. To the south of the caldera, there is no sign of attenuation on the recorded events.

3.3 V_s/V_p analysis and reservoir characterization

It is important to know the reservoir condition before committing a field to more expensive exploration drilling. Advance reservoir knowledge will aid in decision making whether to go ahead with exploration drilling and the drilling techniques to be used. This is because a geothermal system life span depends on the dominant fluid phase and management strategies such as injection/re-injection adopted right from the start of extraction. Phase separation, which is a function of temperature, pressure and fluid saturation, produces different classes of vapour plus fluid and vapour only dominated systems. It enhances convection as it removes heat more efficiently than fluid circulation alone while at the same time, accelerating cooling of the heat sources.

It can also cause rapid expansion of the fracture network, thus enhancing permeability. Thus geothermal systems in which phase separation has not occurred persist ten times longer than those with evidence of phase separation (Ito et al., 1979). For sustainable geothermal power production, it is necessary to know whether phase separation has taken place and the rate as it has implications on reservoir management strategies to be adopted.

O'Connell and Budiansky (1995) have shown that a rock's bulk modulus is affected by the degree of water saturation. The ratio of P-wave velocity to the S-wave velocity (Vp/Vs) increase with pressure increase and temperature decrease from vapour saturated (low pore-pressure) conditions to liquid saturated (high pore-pressure) conditions (Ito et al., 1979).

Studies on these ratios have been contacted in different geothermal fields (McEvilly et al., 1978; Majer and McEvilly, 1979; Combs, 1980; Julian et al., 1996; Simiyu, 1999; Simiyu and Malin, 2000). These studies show that water dominated systems such as East Mesa (California), Cerro Prieto (Mexico), and Olkaria North East (Kenya) have high values 1.7-2. These fields also have low reservoir draw down during exploitation. Steam dominated fields such as Geysers, Coso Hot Springs (California) and Olkaria East (Kenya) have low values, 1.5-1.7 and high reservoir draw-down.

Vp/Vs ratios are known to be sensitive to phase changes in geothermal systems. Water and steam filled pore spaces affect both P and S wave transmission differently. Vp/Vs ratios normally increase from vapour saturated (low pore pressure) condition to liquid saturated (high pore pressure) condition. It is also known that S waves are more adversely affected by anisotropy than P waves and thus Vp/Vs ratios are also expected to vary with azimuth. This is important in delineating geological structures with contrasting physical properties within the reservoir. The highest Vp/Vs ratios were mainly for earthquakes outside the caldera and most of them were for earthquakes from the northeast and the western edge of the area. The caldera, Olbanita area and Northwest areas have the lowest average ratios while the far NE, SW, SE and the area outside the caldera have the highest ratios. This implies that the low ratio areas in the caldera could be having the highest temperature, highly fractured and vapour dominated.

3.4 Hazards analysis

3.4.1 Seismic/earthquake risks

A cumulative magnitude frequency distribution was plotted for the whole area. Earthquakes within the centre of the network with accurate picks (quality 0 & 1) were chosen and checked to ensure that they were not clipped. The cumulative magnitude-frequency relation was plotted for these earthquakes. The magnitude-frequency relation in a particular area obeys the following relation;

$$\text{Log}_{10}\, N = a - bM_c \qquad (5)$$

where, N =the number of earthquakes with a magnitude at least M_c; and
a = is related to the length of time under consideration, normalized to 1 year.

Most of the earthquakes with magnitude 1.5 and more are on the periphery of the geothermal field and outside. This implies that stresses within the geothermal field are being released at a different rate to the surrounding areas.

This is consistent with the regional stress analysis studies (Sass and Morgan, 1987) that suggest that the stress along the rift floor is released by micro-seismic activities in geothermal areas but by larger earthquake sequences along the rift boundary faults. This means that the physical-chemical effects of high temperature and fluids-rock interaction have weakened the crust in the geothermal area.

The value of 'b' parameter in the relationship is relatively high at around 1.05. This implies that the reservoir rocks are in a low stress state with less likelihood of a large earthquake occurring within this volume of the rocks within the field than outside. This value is within the limits usually found within geothermal fields (McEvilly, 1985). The high value implies that there is high heat flow and stress is being released through a high frequency of small magnitude earthquakes.

The corresponding 'a' value is 3.4, which gives a magnitude-frequency expression in equation 5 as; $\text{Log}_{10}\, N = 3.4 - 1.05M_c$. This expression is used to predict the potential for a number (N) of different sized magnitude (M_c) earthquakes occurring within the study area.

Although monitoring of seismic activity in an area requires to be carried out for many years to be able to assess the seismic risk potential, this expression was used to calculate a preliminary risk of potential destructive magnitude $M_c > 5$ earthquake occurring within the geothermal field. The calculations yielded predictions given in table 3.1;

TABLE 3.1: Predicted earthquake risk analysis in the Menengai area

$M_c > 3$	1 event	every 7 months	not felt	not destructive
$M_c > 4$	1 event	every 6.3 years	slightly felt,	not destructive
$M_c > 5$	1 event	every 71 years	moderately felt	destructive
$M_c > 6$	1 event	every 794 years	strongly felt	very destructive
$M_c > 7$	1 event	every 9,000 years	extreme	disastrous

This shows that there is no likelihood of a destructive magnitude $M_c > 5$ earthquakes occurring within the study area. This is because most of the energy is being released through the occurrence of many small earthquakes.

3.4.2 Volcanic eruption risks

Menengai area is located within a region of a triple rift junction that is considered to overly a mantle plume (Burke & Dewey, 1973). The surface is comprised of several eruptive volcanoes with caldera collapses and concentrations of tectonic grid faulting (block and fissure faults). These are characteristic of extension faulting associated with spreading at crustal boundaries. Such areas are tectonically unstable and are thermally privileged with huge supply of magma reservoirs.

Our study shows that a large magma body underlies the Menengai area that extends from within the caldera to the NE walls and the Olbanita area. That means that in the event of an eruption, it might not be confined within the existing caldera. Shear wave attenuation and the brittle –ductile transition depth show that the molten material is at a very shallow depth of about 6 to 8 km. At such a depth, any new injection into the magma chamber from the mantle will lead to volcanic eruptions. Velocity ratio analysis shows that this is a very strong heat source, which is unlikely to be cooling.

Geochemical analysis by Omenda (1998) show that the magmatic materials of this volcanic centre (including Olkaria, Longonot and Suswa) is highly evolved and is therefore bound to be explosive thus its ejected material cover expansive areas. The fact that it is located within a triple junction means that there is a rich supply of mantle derived magmatic gases that are bound to be very poisonous.

Considering the high human population, commercial activities, farming and animal conservation within the area. There is need to have a continuous monitoring of the magma activities beneath the area by seismic methods and gas chemistry. Such monitoring will form a basis for an early warning system.

4. DISCUSSION

The distribution of epicentres in Menengai show that more intense, smaller and shallower events are prominent in the centre of the field and larger, deeper events on the periphery. Seismic activity gaps mapped within the Menengai prospect mark zones of hot magma intrusions that have raised the temperature.

Ray paths from deep events through the centre of the field show that there is a deep attenuating body directly beneath the central part of the caldera structure and taking on geometry with a NE-SW major axis that is consistent with the structure. At shallow depth, the location of individual bodies occur along NNW-SSE and NE-SW trends that could be controlled by the Nyanza rift and Kenya rift axial fault structures along which there has been magma injection. This shows very clearly that the arcuate nature of structure within the Menengai Volcanic Complex can be attributed to caldera-related activities and Nyanza rift. There could also be limited influence from strike slip fault interaction with the rotation of regional stress fields. The lateral extent of the heat sources for the geothermal system at Menengai could be confined within the caldera at deeper level.

The developed Vp/Vs ratios show the caldera areas to have lower velocity ratio formations with deeper horizons suggesting high temperature, low pore pressure and vapour dominated system A decrease in P-wave velocity with constant S-wave velocity results from a change in the compressibility of the rocks. Intense fracturing of the upper crust in areas of high heat flow is a plausible explanation based upon analysis of these data. The values are higher to the SW, SE, East, NE and NW because it could be a possible recharge zone for the system. This zone is water saturated with less steam and high water saturation pressures within the reservoir.

Theoretical estimates of the Vp/Vs anomalies that would be caused by differences in pore-fluid phase, temperature, and pore pressure, for rocks with different porosity. For zero porosity, the Vp/Vs ratio

equals that of the rock matrix, and the effects of temperature and pressure are much too small to contribute significantly to the observed anomaly. At finite porosity, the compressibility of the pore fluid strongly affects Vp/Vs. The largest effect is caused by the contrast between liquid and steam. On the other hand, the dependence of vapour's compressibility on temperature is also important. The Vp/Vs anomaly is caused probably by vapour domination. This means that the reservoir is vapour rich in its natural state, while the surrounding rocks of the area outside the inner caldera, especially to the south, NE and west is not. This means that the reservoir has a Vp/Vs anomaly before exploitation. The magnitude of this anomaly can be explained entirely by the difference between water vapour in the reservoir and liquid water in the surrounding rocks.

We have therefore been able to map in Menengai a low-pressure/high temperature steam dominated reservoirs region and a high-pressure water dominated reservoir region.

5. CONCLUSIONS

This study has been able to show that there exists a high temperature geothermal system within the Menengai prospect area that can be exploited to generate electricity. Figure 5.1 shows a summary of results from this study and proposed sites for drilling of the production wells.

5.1 The heat source

This study has mapped the spatial seismic intensity, hypocenter distribution, event magnitude, depth of clusters with time and shear wave attenuating structures. All these results, combined with gravity and magnetics show that a large high temperature body at a depth of at least 6.5 km beneath the caldera and 7.5 Km beneath Olbanita area underlies the Menengai volcanic area.

5.2 Reservoir size, fluid phase, and characteristics

Three-dimensional seismic travel-time tomography of the prospect shows a strong Vp/Vs anomaly that corresponds to the most highly intruded part of the field. This anomaly indicates low pore pressure and dry conditions caused by boiling of pore water due to limited fluid inflow. The low values correspond to a decrease in P-wave velocity due to high heat flow, fracturing of rocks and steam saturation.

The reservoir is mainly steam dominated in the central caldera area, the immediate NE and part of the NW within the caldera. It is water dominated to the MNW at Olbanita. The geothermal reservoir area that is based on the 1.71 velocity ratio contour (Figure 5.1) is about 80 km^2 and the main productive zone would be in the depth range of 1200-2500 m.

5.3 Recharge for the system

A major water-dominated area has been mapped mainly to the NE from the Aberdare escarpment and a minor one to the NW of the caldera system along the rift axis. Other minor recharge regimes are from the SW, SE and west. These water-dominated areas represent the cold fluid recharge corridors for the geothermal system.

5.4 Sitting of wells

Figure 5.1 show three proposed drill sites. One is within the caldera, in the low velocity ratio zone and above the mapped high temperature heat sources. The second one is at Olbanita where a buried caldera has been inferred (Mungania, 1999). And the third one is on the caldera wall to the NE but has been sited outside the rim in order to validate the caldera control on the geothermal system. Drilling of these wells will validate the method and give a clear indication of the reservoir size and heat source

estimates. This study suggests that the high temperature system is controlled by the calderas and any future development should be confined in the area defined by them.

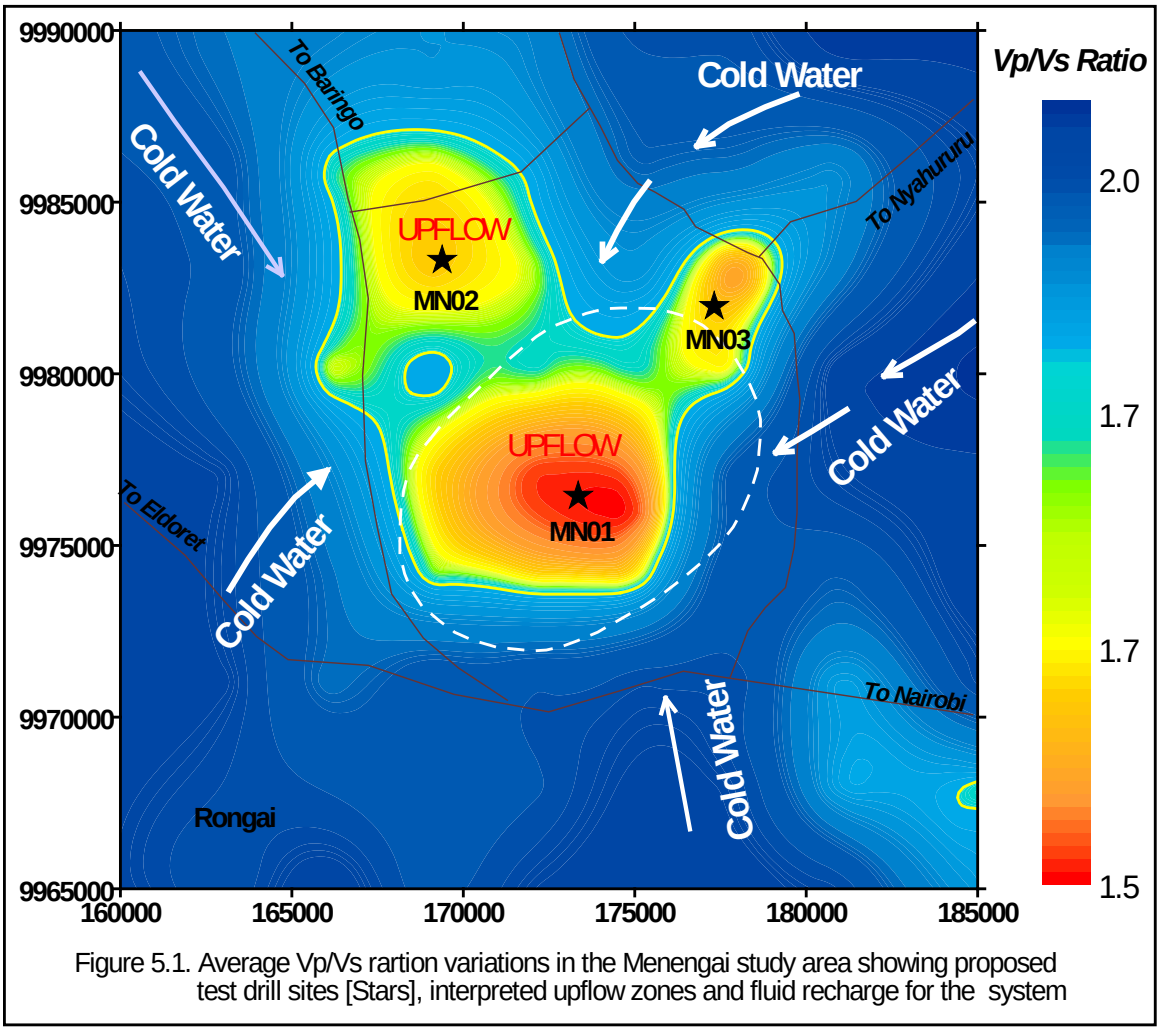

Figure 5.1. Average Vp/Vs rartion variations in the Menengai study area showing proposed test drill sites [Stars], interpreted upflow zones and fluid recharge for the system

5.5 Earthquake risk analysis for the area

The value of 'b' parameter in the relation is high around 1.05, which is within the limits found in geothermal fields. A high value implies that there is high heat flow and stress is being released through a high frequency of small magnitude earthquakes. This leads to reservoir rocks being in a low stress state with less likelihood of a large earthquake occurring within this volume of rocks. The magnitude thresh-hold for this area is M_c =1.4. This shows that there is less likelihood of having a large destructive earthquake within the study area.

5.6 Volcanic risk assessment

Heat source analysis shows the existence of a high temperature molten body directly beneath the Menengai volcanic centre. During this study, there has been no direct monitoring of magma activity. However, the presence of this large magma body beneath a central volcano such as Menengai is a major risk. This volcano has also a unique volcano-tectonic origin (plume driven triple junction), which means that it can release large volumes of ejector and mantle derived poisonous gases.

The risk assessment for this area is made in view of the expansion in the area's rich agriculture, wildlife conservation (Nakuru Park) and commercial activities in Nakuru town. The influx of people into the area surrounding the volcanic centre makes them directly exposed to these high potential volcanic hazards. Since we cannot stop a volcanic eruption but we can predict it, there is need to have a volcano-seismic risk-monitoring program for the area. This will be important for continuous resource evaluation and risk monitoring that can form a basis for an early public warning system

.

REFERENCES

Burke, K., and Dewey, J. F. 1973. Plume generated triple junctions: Key indicators in applying plate tectonics to old rocks. Journal of Geology, 81, 406-433.

Chen, W. P., and Molnar P., 1983. Focal depths of intra-continental and intra-plate earthquakes and their implications for the thermal and mechanical properties of the lithosphere. J. Geophys. Res., 88, 4183-4214.

Clarke, G.C., Woodhall, D.G., Allen, D. and Darling, G. Geological, 1990.Volcanological and Hydrogeological Controls on the Occurrence of Geothermal Activity in the Area Surrounding Lake Naivasha, Kenya. BGS/GK report, 125p.

Combs, J., 1975. Geophysical Techniques in Geothermal Exploration. In Proceedings of the 2nd Symposium on the development and use of Geothermal Resources. Vol. 1 95-99.

Combs, J., 1980. Heat flow in the Coso geothermal area, California. J. Geophys. Res., 85, 2411-2424.

Fairhead, J. D. and Stuart, G. WS. 1982. The seismic activity of the East African Rift system and comparison with other continental rift, In G. Palmason (editor), Geodynamic series AGU, Washington DC, 8, 41-61.

Foulger, G.R., Long, R.E., and Einarsson, P., 1989. Implosive earthquakes at the active plate boundaries in Iceland, Nature, 337: 640-642.

Hamilton, R.M., Smith, B.E., And Knapp, F., 1973. Earthquakes in geothermal areas near Lake Naivasha and Lake Hannington. Unpublished report by the United States Geological Survey for the UNDP/EAPL, pp37.
Henry, W.J., Mechie, J., Maguire, P.K.H., Khan, M.A., Prodehl, C., Keller, G.R. and Patel, J., 1990. A seismic investigation of the Kenya Rift Valley. Geophys. J. International, 100: 107-130

Ito, H., DeVibriss J., and Nur A., 1979. Compressional and Shear waves in saturated rock during water-steam transition. J. Geophys. Res., 84, 4731-4735.

Julian, B. R., Ross A., Foulger G. R., and Evans J. R. 1996. Three –dimensional seismic image of a geothermal reservoir: The Geyser, California. Geophys. Res. Lett. 33, 685-688.

Lee, W.H.K., Bennett, R.E. and Meagher, K.L., 1972. A method for estimating magnitude of local earthquakes from signal duration. United States Geological Survey, Open File Report, 37pp.

Macdonald, R., 1994. Petrological evidence regarding the evolution of the Kenya Rift Tectonophysics, 236: 373-390.

Majer, E. L., and McEvilly T. V., 1979. Seismological investigations at the Geysers geothermal field. Geophysics 44, 246-269.

McEvilly, T.V, Schechter, B., and Majer, E. L., 1978. East Mesa seismic study. Annual Report, Earth Sciences Division, Lawrence Berkeley Laboratory, University of California. 26-28.

Meissner, R and Strehlau, J., 1982. Limits of stress in the continental crust and their relation to depth-frequency distribution of shallow earthquakes. Tectonics, 1, 73-89.

Mungania, J. 1995. Tephra deposits in Olkaria and the surrounding areas. A KPC unpublished report. 7 pp.

Omenda, P. A., 1998. The geological structure of the Olkaria geothermal field. Geothermics, 19: 125-130.

Simiyu S. M, and Malin P. E., 2000. A volcano-seismic approach to geothermal exploration. 5th World Geothermal Congress, Morioka, Japan, WGC2000-TR-1345.

Simiyu S. M., and Novak, O 1994. Kenya Rift International Seismic Project (KRISP) 1994 seismic profiling experiment. Eos, Trans. Am., Geophys. Union. 75: 44, 664-665.

Simiyu, S. M., Omenda, P. A., Anthony E. Y., and Keller, G. R., 1995. Geophysical and geological evidence for the occurrence of shallow magma intrusions in the Naivasha sub-basin of the Kenya Rift. EOS, Trans. Am. Geophys. Union.76, 46, 257-258.

Simiyu S. M., and Keller G. R., 1997. Integrated interpretation of the East African plateau based on gravity anomalies and recent seismic studies. Tectonophysics 278: 327-352.

Simiyu S. M., 1998. Seismic and gravity interpretation of the shallow crust structure along the KRISP 94 line G in the vicinity of the Kenya Rift Valley. J. African Earth Sciences, 27: 367-381.

Simiyu S. M., and Keller G. R., 2000. Micro-seismic monitoring within the Olkaria geothermal area, Kenya. J. Volc. Geoth. Res., 95, 197-208.

Simiyu S. M., 2000. Geothermal reservoir characterization: Application of micro-seismic activity and seismic wave properties. J. Geophys. Res., 105, NO. B6, 13,779-13,795.

Simiyu S. M and Keller G. R., 2001. Geophysical interpretation of the upper crust structure of the southern Kenya Rift. Geophys. J. Int.

Walter, A. W., and Weaver C. S., 1980. Seismic activity of the Coso Range, California. J. Geophys. Res., 85, 2441-2458.

Wheildon, J., Morgan, P., Williamson, K. H., Evans, T. R., and Swanberg, C. A., 1994. Heat flow in the Kenya rift zone. Tectonophysics, 236, 131-149.

Young P., Maguire P., Laffoley A., and Evans J., 1991. Implications of the distribution of seismic activity near Lake Bogoria in the Kenya rift. Geophys. J. Int., 105, 665-674.